Published in final edited form as:
Cancer Lett. 2013 January 1; 328(1): 55–64. doi:10.1016/j.canlet.2012.09.011.

Expression of Tax-interacting protein 1 (TIP-1) facilitates angiogenesis and tumor formation of human glioblastoma cells in nude mice

Miaojun Han[a,b,c], **Hailun Wang**[a], **Hua-Tang Zhang**[b], and **Zhaozhong Han**[a,d,e,*]

[a]Department of Radiation Oncology, School of Medicine, Vanderbilt University, Nashville, TN 37232, USA

[b]Key Laboratory of Animal Models and Human Disease Mechanisms of the Chinese Academy of Sciences & Yunnan Province, Kunming Institute of Zoology, Yunnan, China

[c]Graduate School, Chinese Academy of Sciences, Beijing, China

[d]Department of Cancer Biology, School of Medicine, Vanderbilt University. Nashville, TN 37232, USA

[e]Vanderbilt-Ingram Cancer Center. Nashville, TN 37232, USA

Abstract

Glioblastoma is the most common and fatal type of primary brain tumors featured with hyperplastic blood vessels. Here, we performed meta-analyses of published data and established a correlation between high TIP-1 expression levels and the poor prognosis of glioblastoma patients. Next, we explored the biological relevance of TIP-1 expression in the pathogenesis of glioblastoma. By using orthotopic and heterotopic mouse models of human glioblastomas, this study has characterized TIP-1 as one contributing factor to the tumor-driven angiogenesis. *In vitro* and *in vivo* functional assays, along with biochemical analyses with microarrays and antibody arrays, have demonstrated that TIP-1 utilizes multiple pathways including modulating fibronectin gene expression and uPA protein secretion, to establish or maintain a pro-angiogenic microenvironment within human glioblastoma. In conclusion, this work supports the hypothesis that TIP-1 represents a novel prognostic biomarker and a therapeutic target of human glioblastoma.

Keywords

TIP-1; PDZ; glioblastoma; angiogenesis; fibronectin; uPA 1

[*]**Corresponding author:** Department of Radiation Oncology School of Medicine, Vanderbilt University 1301 Medical Center Drive, B902 TVC Nashville, TN 37232 Phone: (615) 322 1037 zhaozhong.han@vanderbilt.edu.

Conflict of Interest: All the authors declared no conflict of interest related to this work.

Introduction

Glioblastoma (also known as glioblastoma multiforme or GBM, WHO grade IV malignant glioma) is the most common and fatal type of primary brain tumor. These tumors are featured with highly invasive growth into normal surrounding tissues and a vasculature-rich tumor mass. Even with the most aggressive treatment including surgical resection of as much of tumor as possible, concurrent or sequential chemoradiotherapy, antiangiogenic therapy and symptomatic management, newly diagnosed patients with glioblastoma typically have a survival time of about 16 months [1]. Extensive studies have identified dozens of genetic or epigenetic factors that control the aggressive tumor growth and treatment resistance [2; 3; 4; 5].

TIP-1, also known as Tax1-binding protein 3 (Tax1bp3) and glutaminase-interacting protein (GIP), is a small (124 amino acids in human and mouse) and conserved protein containing single PDZ (PSD-95/DlgA/ZO-1) domain [6]. TIP-1 involves in a wide spectrum of biological processes through selective protein interactions, such as beta-catenin [7], brain-specific angiogenesis inhibitor 2 [8], rhotekin [9], HPV16 E6 [10], HTLV-1 Tax [11], ARHGEF16 [12], potassium channel Kir2.3 [13], and glutaminase [14]. TIP-1 has been reported to regulate gastrulation movements during zebrafish embryo development [6]. In Madin-Darby canine kidney (MDCK) cells, TIP-1 modulates trafficking of intracellular proteins and contributes to the establishment of cell polarity [13]. TIP-1 is required for the HPV16 E6 oncoprotein-induced cell transformation [10]. TIP-1 has also been shown with inhibitory function on the transcriptional activity of beta-catenin and colon cancer cell proliferation [7]. However, the biological roles of TIP-1, especially in tumorigenesis, remain largely unclear.

Our previous studies have documented the elevated TIP-1 expression levels in human invasive breast cancers [15]. It was found that TIP-1 expression in human breast cancer cells contributes to cellular adhesion to extracellular matrix, invasion and pulmonary metastasis in mouse models. In this study, we further expanded the association of TIP-1 expression with cancer progression to human glioblastoma. Meta-analyses of published data indicated a correlation between the elevated TIP-1 expression levels and the poor prognosis of patients with glioblastoma. By using orthotopic and heterotopic mouse models of human glioblastomas, we have identified a novel function of TIP-1 protein in the early stages of glioblastoma formation. The data demonstrated that TIP-1 facilitates tumor-driven angiogenesis and promotes tumor formation of human glioblastoma cell lines in nude mice. Biochemical analyses with microarrays and antibody arrays further suggested that TIP-1 might utilize multiple pathways including modulating fibronectin gene expression and uPA protein secretion, to establish or maintain a pro-angiogenic tumor microenvironment. This work, along with our ongoing studies, supports the hypothesis that TIP-1 represents a novel therapeutic target and prognostic biomarker of human glioblastoma.

2. Materials and methods

2.1. Antibodies and reagents

Rabbit anti-human TIP-1 was produced as described previously [16]. Antibodies against IGFBP3 and SPP1 were purchased from Santa Cruz Biotechnology (Santa Cruz, CA). Antibodies recognizing FN1 were from Epitomics (Burlingame, CA). Anti-Ki67 antibody was from Abcam (Cambridge, MA) and the TUNEL assay kit from Promega (Madison, WI). HRP- or fluorescence-labeled secondary antibodies were from Invitrogen (Carlsbad, CA). Anti-actin antibody and chemicals were purchased from Sigma (St. Louis, MO) unless otherwise stated.

2.2. Cell culture, RNA interference and cell transfection

Human glioma cell lines D54 or U87 were obtained from Dr. Yancie Gillespie (University of Alabama-Birmingham, Birmingham, AL) and ATCC (Manassas, VA), respectively. All the cell lines were genetically and morphologically verified by the provider before the experiments. Constructs expressing validated small hairpin RNA (shRNA) were purchased from Sigma, including two TIP-1-specific shRNAs (TIP-1 shRNA #1: 5′-GGCTAACAGCTGATCCCAA-3′, TIP-1 shRNA #2: 5′-GCAAAGAGTTGAAATTCACAA-3′) matching different regions of the human TIP-1 mRNA transcript. A non-targeting sequence was used as a negative control. Two validated small interfering RNAs (siRNAs) for FN1 (FN1 siRNA-1: 5′-CAAUUACACUGAUUGCACU-3′ and FN1 siRNA-2: 5′-CACUUAUGAGCGUCCUAAA-3′) were purchased from Sigma. RNAi MAX (Invitrogen) was used for siRNA transfection by following the manufacturer's instructions. The RNAi-tranfected cells were used for experiments 48-72 hours after the transfection. Transfection of the cells with the recombinant plasmids and formation of stable clones were achieved by standard protocols [17]. Protein expression level was detected by western blot analysis of whole cell lysates with the specific antibodies.

2.3. Tumor growth studies in mouse models

Tumor formation and growth were studied with intracranially and subcutaneously implanted xenograft models. In the intracranially implanted xenograft model, human glioblastoma cell lines (D54 or U87 with or without TIP-1 knockdown) were genetically modified with a luciferase-expressing construct (Addgene, Cambridge, MA). A total of 2×10^4 cells in 20 μl of phosphate-buffered saline (PBS) were injected 3 mm deep (from the skull surface) into the right burr hole of FoxN1-null nude mice (Harlan Laboratories, Prattville, AL). Tumor formation and growth were monitored every three days by bioluminescence imaging (BLI) [18] using an IVIS 200 imaging station (Caliper Life Sciences, Hopkinton, MA). The bioluminescence signal was acquired 12 minutes after intraperitoneal injection of luciferin (D-luciferin potassium salt, 150 mg/kg, Caliper Life Sciences). In the subcutaneous xenograft model, 5×10^5 D54 cells, with or without TIP-1 knockdown, were resuspended in 200 μl of PBS for subcutaneous injection into the flanks of FoxN1-null mice. Tumor sizes were measured with calipers every other day until the tumor volume reached 700 mm^3. Tumor tissues were resected for immunohistochemical (IHC) staining to determine cell death, cell proliferation and blood vessel formation. All the animal studies were approved by the Institutional Animal Care and Use Committee (IACUC) at Vanderbilt University.

2.4. Matrigel-plug assay

The impact of TIP-1 and fibronectin on D54 tumor angiogenesis were studied with matrigel-plug assays. Briefly, 5×10^5 D54 cells were resuspended in 150 μl PBS and mixed with 350 μl ice-cold Matrigel (BD Biosciences, Rockville, MD). The cell/matrigel mixture was subcutaneously injected into the hind limbs of FoxN1-null mice. In order to minimize the variations between animals, cells with a specific gene manipulation and those with vector control were implanted in the same animal, respectively. Roles of fibronectin in TIP-1 regulated tumor angiogenesis were also studied by adding the purified recombinant fibronectin protein (25 μg/ml in PBS, Sigma) to the matrigel mixture with TIP-1 knockdown cells. To visualize the functional blood vessels within the matrigel-plugs, 150 μl of FITC-dextran (25 mg/ml, 2000 kD, Sigma) were injected through tail veins 15 minutes prior to sacrificing animals. The matrigel-plugs were removed for examination with a confocal fluorescence microscope, and FITC signals within the matrigel plugs were quantified with ImageJ software (http://rsbweb.nih.gov/ij/index.html). The matrigel-plugs were also used to extract tumor cells for quantification of angiogenic factors with antibody array or fixed with formaldehyde and embedded in paraffin for IHC staining [19].

2.5. Immunohistochemistry

Five (5) μm of paraffin-embedded tissue sections were dewaxed in xylene and rehydrated at gradient concentrations of ethanol (100%, 95%, 90%, 80%, 70% in PBS, 5 minutes each solution). Antigen retrieval was performed by incubating the slides with 100 mmol/L sodium citrate solution (pH 6.0) for 20 minutes. Tumor blood vessels were stained with anti-vWF antibody (Vector Labs, Burlingame, CA). Cell proliferation and apoptosis were detected by staining with anti-Ki67 antibody and a TUNEL assay kit, respectively. Positively stained cells and total cells per field were counted to calculate the proliferative index (Ki67) and the apoptotic index (TUNEL).

2.6. Endothelial cell migration and tubule formation assays

Angiogenic factors secreted by D54 human glioblastoma cells were analyzed with HUVEC migration and tubule formation assays. Briefly, a monolayer culture of D54 cells (with or without TIP-1 knockdown) at 75% confluence was washed with cold PBS three times before being incubated with serum-free DMEM/F12 media for 24 hours. The pre-conditioned media were filtered to remove cell debris for HUVEC migration and tubule formation assays. The HUVEC migration assay was performed using 8-μm porous Boyden chambers (Corning Life Science, Lowell, MA) according to the manufacturer's instructions. Prior to the migration assays, HUVECs were starved in serum-free medium overnight. Approximately 20,000 disaggregated HUVECs were seeded into the insert chambers with serum-free medium. Pre-conditioned media were added to the lower chambers. After 5 hours, the cells that stayed on the top of the membrane were removed with cotton swabs, and the cells that migrated to the bottom of the membrane were stained with DAPI and counted under a fluorescence microscope. In the tubule formation assay, 8,000 disaggregated HUVECs were seeded into each well of a 96-well plate that had been coated with 50 μl Matrigel (BD Biosciences) and contained 200 μl preconditioned medium. Tubule-like structures were imaged by the use of a phase contrast microscope after incubation at 37°C for 5 hours. Images were taken from at least 4 microscopic fields from each well, and nodes with more than 3 branches were counted as tubule networks.

2.7. Antibody arrays and ELISA quantification

Human angiogenesis array kits (R&D, Minneapolis, MN) were utilized for semi-quantification of the angiogenic factors within *in vitro* and *ex vivo* samples. The *in vitro* samples were pre-conditioned media from D54 cells with or without TIP-1 knockdown as described above. *Ex vivo* samples were prepared by recovering tumor cells from matrigel-plugs after 8 days of the matrigel-plug implantation, incubating the tumor cells with serum-free DMEM/F12 medium for 24 hours, and collecting the pre-conditioned media by filtration to remove the cell debris. Staining of the membranes with arrayed antibodies against human-originated angiogenic factors was conducted by following the manufacturer's instructions. Signal intensity was semi-quantified upon the histograms of scanned films. All of the data were normalized to the inner controls. uPA concentrations in the pre-conditioned media were determined by use of a uPA ELISA kit from Syd Labs (Malden, MA) according to the manufacturer's instructions.

2.8. RNA isolation, microarray profiling, and quantitative RT-PCR(qRT-PCR)

RNA transcripts from D54 cells were isolated by the use of a RNAqueous Kit (Ambion, Austin, TX) as instructed by the manufacturer. The quality of the RNA was validated by agarose gel electrophoresis. One μg of total RNA was used for cDNA synthesis with a QuantiTect reverse Transcription Kit (QIAGEN, Valencia, CA) in microarray profiling and quantitative reverse transcriptase PCR (qRT-PCR). Gene expression profiling was performed using Affymetrix Gene Chips at Vanderbilt's Functional Genomics Shared

Resource (FGSR). Heatmaps of gene expression were generated using Cluster and TreeView (Michael Eisen, Stanford University). Hierarchical clustering of genes was performed using average linkage and Pearson correlation distance matrices. The functions of clustered genes were analyzed by GoMiner software [20]. The qRT-PCR was performed using a QuantiFast SYBR Green PCR Kit (QIAGEN) according to the manufacturer's instructions on a Bio-Rad CFX96 qRT-PCR system (Bio-Rad, Hercules, CA). Specific primer sets for FN1, SPP1, IGFBP3 and GAPDH were purchased from QIAGEN. The $\Delta\Delta C_T$ method was applied to calculate the relative gene expression levels [5].

2.9. Statistics

Meta-analysis was based upon published microarray data sets [5; 21]. To compare TIP-1 expression levels within human malignant gliomas of various stages, one dataset [21] including 157 cases of primary human malignant gliomas of the grade II to IV, and 23 cases of non-tumor normal human brain samples was reanalyzed. To determine the prognostic value of TIP-1 expression level, 55 cases of glioblastoma (WHO grade IV) patients [5] were ranked upon TIP-1 expression levels. Subjects within the top 35% (20 cases) of the TIP-1 expression levels were classified as "TIP-1 high", while those within the bottom 35% (20 cases) of the TIP-1 expression level were classified as "TIP-1 low". Survival probability were plotted with the Kaplan-Meier method and compared with a log-rank test. The Student's *t* test was used to determine the statistical significance unless otherwise stated. All quantitative data was presented as mean +/− standard deviation (SD). For all analyses, a *p* value less than 0.05 was considered significant. For microarray data, False Discovery Rate (FDR)-adjusted *p*-value was calculated upon Benjamini correction method [22].

3. Results

3.1. High levels of TIP-1 expression correlate with the poor prognosis of human glioblastoma

Comparison of TIP-1 expression levels in clinical specimens upon the previously published microarray data [21] revealed significantly elevated TIP-1 expression levels in the high-grade gliomas (grade III, n=31; grade IV, n=81) compared to those in low-grade gliomas (grade II, n=45) or normal brain tissue (n=23) ($p<0.05$) (Fig. 1A). Analysis of microarray data from patients with WHO grade IV gliomas (glioblastoma) indicated that TIP-1 expression levels are independent of age or gender of the glioblastoma patients (Supplementary Figs. 1A and 1B). Survival probability analysis of those glioblastoma patients [5] indicated that the TIP-1 expression level is a putative prognostic biomarker, as the glioblastoma patients with high TIP-1 expression levels (top 35% of TIP-1 expression levels, 20 cases) experienced a significantly shorter survival time ($p=0.0274$) after diagnosis than those patients with tumors expressing relatively low levels of TIP-1 (bottom 35% of TIP-1 expression levels, 20 cases) (Fig. 1B). Similar results (Supplementary Fig. 1C) were also observed by analyzing another independent data set [23].

3.2. TIP-1 knockdown within human glioblastoma cell lines delays tumor formation in nude mice

The role of TIP-1 expression in tumor formation and growth of human glioblastoma were studied with two established human glioblastoma cell lines (D54 and U87) in mouse models. TIP-1 expression in those cell lines was downregulated with recombinant lentiviruses encoding small hairpin RNA (shRNA) sequences that had been validated with specificity to human TIP-1 mRNA transcripts [16]. To avoid off-target artifacts, two independent shRNA clones were utilized in this study. TIP-1 knockdown in D54 and U87 cells was verified by western blot analyses of the cell lysates with a TIP-1 specific antibody [16] (inserts of Figs. 2B, C). The cells were infected with luciferase-expressing lentiviruses before implantation

into the right basal ganglia of Foxn1-null nude mice, and tumor cell expansion and growth was monitored by *in vivo* bioluminescent imaging (BLI) and quantified by the light emitted from the luciferase-expressing glioblastoma cells (Fig. 2A). TIP-1 knockdown delayed tumor formation for more than eight days of D54 (Fig. 2B) and U87 cells (Fig. 2C). A similar effect of TIP-1 knockdown on tumor formation was observed in a subcutaneously implanted D54 xenograft model in which tumor size was measured with calipers. Compared to the D54 cells with control shRNA that developed tumors of ~50 mm^3 by day 14 after the tumor cell inoculation, it took around 35 days for the D54 cells with TIP-1 knockdown to grow tumors of the same size (Fig. 2D). in both of the orthotopic and heterotopic models, TIP-1 knockdown had a moderate impact on the tumor growth rate once the tumors started growing beyond a detectable size.

3.3. The delayed tumor formation from TIP-1 knockdown is associated with reduced tumor blood vessel density

To dissect the mechanism(s) by which TIP-1 knockdown delays the tumor formation, tumor tissues were resected 12 days after the tumor cell inoculation in the subcutaneous D54 xenograft model. Ki67 staining showed no significant difference in cell proliferation rate between the control and TIP-1 knockdown D54 tumors (Supplementary Fig. s2A). This result is consistent with *in vitro* quantitative measurement of cell doubling time (Supplementary Fig. s2B). The major differences between the TIP-1 knockdown and control D54 tumors were tumor-associated blood vessel density as detected with vWF staining (Fig. 2E). Accompanied with the significantly reduced blood vessel density in the D54 tumors with TIP-1 knockdown, severe hypoxia and more cell apoptosis were detected (Supplementary Fig. s2A). These results suggest a possible role of TIP-1 in angiogenesis of human glioblastoma.

3.4. TIP-1 knockdown impairs production of angiogenic factors of D54 cells in vitro and in vivo

The role of TIP-1 in tumor-associated angiogenesis was further studied with a matrigel plug assay. A half million D54 glioma cells with or without TIP-1 knockdown were mixed with matrigel (70% final concentration, v/v) and then implanted subcutaneously in the hind limbs of Foxn1-null nude mice. On day 8 after the tumor cell inoculation, FITC-dextran was injected into the lateral tail vein before sacrificing the animals to retrieve the matrigel plugs to visualize the functional blood vessels under a fluorescent confocal microscope. Descriptive images, as well as the number of blood vessels quantified by the fluorescence signal, showed that TIP-1 knockdown significantly impaired blood vessel formation in the matrigel plug assays (Fig. 3A). Tumor blood vessels in the control group had much more intense networks than those in the TIP-1 knockdown groups. Since angiogenesis is driven by multiple angiogenic factors, the impact of TIP-1 expression on the production of angiogenic factors was further studied by using two established *in vitro* methods: a chamber-based endothelial cell migration assay and a matrigel-based tubule formation assay [24; 25]. Serum-free medium was incubated with a monolayer culture of D54 cells with or without TIP-1 knockdown for ~24 hours. Angiogenic factors in the pre-conditioned media were detected upon their capability to induce migration and tubule formation of primary human umbilical vein endothelial cells (HUVECs). Results from both of HUVEC migration (Fig. 3B) and tubule formation (Fig. 3C) assays demonstrated that the pre-conditioned media from control D54 cells contains more (around 2-fold) angiogenic factors than those from D54 cells with TIP-1 knockdown.

3.5. TIP-1 knockdown reduces the secretion of angiogenic factors from glioblastoma cells in vitro and ex vivo

D54 cells from monolayer culture (*in vitro*) or those recovered from matrigel-plugs (*ex vivo*) were cultured in serum-free media overnight before the angiogenic factors secreted into the pre-conditioned media were profiled using human angiogenesis antibody arrays. The results showed that TIP-1 knockdown significantly reduced the secretion of several angiogenic factors from the D54 glioblastoma cells (Fig. 4A). Among the angiogenic factors profiled in this study, secretion of urinary plasminogen activator (uPA), insulin growth factor binding protein 1 and 3 (IGFBP1 and IGFBP3), and human TNF-stimulated gene 14 (TSG14) showed significant decreases after the TIP-1 knockdown in both *in vitro* and *ex vivo* assays ($p<0.05$). In the *ex vivo* assays, the reduced secretion of angiogenic factors from glioblastoma cells with TIP-1 knockdown was more remarkable and even expanded to other angiogenic factors such as angiogenin (ANG), vascular endothelial growth factor (VEGF), fibroblast growth factor 2 (FGF2), transforming growth factor β1 (TGFβ1), and tissue factor (TF) (Fig. 4A), suggesting that host factors might also contribute to the TIP-1-regulated secretion of angiogenic factors from glioblastoma cells. Among those angiogenic factors that were significantly affected by TIP-1 expression, uPA was selected for further validation with a quantitative enzyme-linked immunosorbent assay (ELISA). The result showed a remarkable decrease in uPA secretion upon TIP-1 knockdown in both of D54 and U87 cell lines (Fig. 4B).

3.6. TIP-1 knockdown reduces the expression of fibronectin 1 and other pro-angiogenic factors

To further elucidate the mechanisms(s) by which TIP-1 regulates the production of angiogenic factors, gene expression within D54 cells with or without TIP-1 knockdown was profiled by the use of microarrays. Clustering analysis indicated that the genes affected by the differential TIP-1 expression levels are primary associated with cytoskeleton reorganization, cell morphology, migration and angiogenesis (Supplementary Fig. s3). Among those genes, fibronectin 1 (FN1) [26], integrin beta 3 (ITGB3) [27], insulin-like growth factor-binding protein 3 (IGFBP3) [28], a disintegrin-like and metalloproteinase with thrombospondin motifs 1 (ADAMTS1) [29] and secreted phosphoprotein 1 (SPP1) [30] were downregulated by TIP-1 knockdown in D54 cells (Fig. 5A). The microarray data was supported by quantitative RT-PCR measurements of the mRNA transcripts of FN1, IGFBP3, and SPP1 (Fig. 5B) from D54 cells. However, only FN1 demonstrated a significant and consistent decrease at the protein level after TIP-1 knockdown in multiple human glioblastoma cell lines (Fig. 5C and supplementary Fig. s4A).

3.7. FN1 is involved in the TIP-1 regulated angiogenesis within human glioblastomas

In a matrigel plug assay, supplementing TIP-1 knockdown D54 cells with recombinant fibronectin protein partially reversed the defective tumor blood vessel formation caused by TIP-1 knockdown (Fig. 6A). This observation was consistent to a complementary experiment in which knockdown of FN1 with small interference RNA (siRNA) in D54 glioblastoma cells partially resembled the effects of TIP-1 knockdown on tumor angiogenesis (Fig. 6B). In those experiments, it was also observed that FN1 mainly affected the blood vessels with large-diameter and long branches, in contrast to TIP-1 knockdown which affected those with small-diameter and short branches as well (Fig. 6). These data suggested that, in addition to fibronectin, other factors might also contribute to the TIP-1 regulated angiogenesis in human glioblastoma.

4. Discussion

New blood vessel formation is required for tumor growth beyond a specific size [31]. In fact, anti-angiogenesis or vasculature-targeted therapies have been explored to treat multiple kinds of tumors with some exciting success. Since glioblastoma is characterized by a vasculature-rich structure and an extremely high mortality rate, overwhelming efforts have been made to identify the driving forces behind glioblastoma-associated angiogenesis and explore targeting tumor vasculatures for tumor growth control. This study has provided evidence showing that TIP-1 promotes angiogenesis and tumor formation of human glioblastoma cells in mouse models. Biochemical analyses with microarrays and antibody arrays suggested that TIP-1 might utilize multiple pathways including modulating fibronectin gene expression and uPA protein secretion, to establish or maintain a pro-angiogenic microenvironment.

TIP-1 is conserved protein across several species [6]. In zebrafish, high level of TIP-1 expression was detected in the early stage of embryo development and only in central nervous system thereafter. TIP-1 inhibition impaired the filopodia growth and gastrulation movement [6]. In mammals, TIP-1 expression was detected in both of neurons and astrocytes though the roles of TIP-1 expression in these cells have not been defined yet [32]. This study revealed that TIP-1 expression levels are elevated in the advanced human malignant gliomas, and the elevated TIP-1 expression levels correlate to the prognosis of human glioblastoma. *In vitro* and *in vivo* studies further characterized TIP-1 as one driving force in angiogenesis and tumor formation of human glioblastoma. The oncogenic functions of TIP-1 have also been documented in several other systems. For example, the elevated TIP-1 expression in human invasive breast cancers is essential to cell migration, invasion, adhesion and pulmonary metastasis in nude mice [15]. TIP-1 is a gain of function target of the HPV16 E6 oncoprotein in cell transformation [10]. TIP-1 is required for the cell polarity establishment of epithelial cells through modulating trafficking of intracellular proteins [13]. It was also noted that TIP-1 expression in colon cancer cells suppressed the transcriptional activity of beta-catenin and inhibited cell proliferation [7]. The discrepancy regarding TIP-1's roles in different type of cells might reflect that TIP-1's biological functions largely depend upon the cellular context.

Tumors evolve to drive extracellular matrix (ECM) remodeling through autocrine or paracrine mechanisms to establish or maintain a favorable microenvironment for tumor formation, growth, and metastasis. In this study, it was observed that TIP-1 drives gene expression and protein production for angiogenesis of human glioblastoma. Functional assays and quantitative measurements indicated that TIP-1 knockdown resulted in a reduced production and secretion of angiogenic factors including uPA, TSG14, IGFBP1, IGFBP3 and others. uPA plays crucial roles in modulating ECM to establish a pro-angiogenic tumor microenvironment. Its binding to the corresponding receptor (uPAR) initiates signaling cascades for activating plasminogen, remodeling ECM, and liberating or mobilizing ECM-associated angiogenic factors such as FGF2 and VEGF [33; 34]. Elevated uPA production has been reported in multiple tumor types, and targeting uPA has been proposed to treat tumors. It was also noted that TSG14, IGFBP-1 and IGFBP-3 have been reported to regulate angiogenesis through triggering inflammation or modulating the IGF/IGFR signaling pathway [35; 36]. Microarray profiles indicated that the majority of those genes that were significantly affected by TIP-1 expression are associated with cytoskeleton reorganization, cell morphology, migration, and angiogenesis. Among those TIP-1 regulated genes, fibronectin was particularly interesting since its interaction with integrins expressed on the plasma membrane promotes cell adhesion, triggers signaling pathways for cell survival and proliferation, and recruits host-derived growth factors or stromal cells. In fact, we observed that human glioblastoma cells expressing TIP-1 had an improved cell adhesion to plastic

plates while compared to those cells with TIP-1 knockdown (Supplementary Fig. s2C), that probably dues to the production of FN1 and might contribute to the cell survival in the early stage of tumor cell inoculation in nude mice. FN1 is a key ECM protein that has been well established as a modulator of physiological and pathophysiological angiogenesis through promoting endothelial cell migration and survival [26]. Deletion of FN1 caused severe defects in angiogenesis and vascular development [27]. In this study, TIP-1 knockdown reduced fibronectin expression in multiple human glioblastoma cell lines at both the gene and protein levels. Supplementing the TIP-1-deficient glioblastoma cells with recombinant fibronectin partially restored its impaired tumor blood formation in matrigel-plug assays, whereas fibronectin knockdown in glioblastoma cells, to some extent, resembled the impact of TIP-1 knockdown on the tumor angiogenesis. Those discoveries are clinically relevant since FN1 expression and uPA secretion were also significantly reduced after TIP-1 knockdown within two primary human glioblastoma cell lines (GBM6 and GBM43) [37; 38] that were passaged as xenografts in a limited number after isolation from clinical specimens (Supplementary Fig. s4). Based on these data, we envision that TIP-1 facilitates establishing or maintaining a pro-angiogenic microenvironment through regulating gene expression and protein secretion for angiogenesis and tumor formation.

Fibronectin is a transcriptional target of β-catenin [39] and it in turn modulates the transcriptional activity of β-catenin [40]. It has been reported that TIP-1 inhibits β-catenin's transcriptional activities in colon cancer [7]. However, it seems unlikely that β-catenin is involved in the TIP-1-regulated fibronectin gene expression in glioblastoma cells. Microarray profiling clearly showed that c-Myc, cyclin D1 and several other transcriptional targets of β-catenin were not affected by TIP-1 expression within glioblastoma cells. TIP-1 interacts with Rho effector Rhotekin and modulates Rho signaling to serum response element (SRE) [9]. In that report, TIP-1 itself also demonstrated a weak but significant activity towards SRE-controlled gene expression. It was reported that fibronectin expression is serum-inducible [41; 42], it would be interesting to study whether TIP-1 affects fibronectin expression in glioblastoma cells through the Rho-regulated SRE. Regarding the impact of TIP-1 expression on the production of angiogenic factors, most of these angiogenic factors were not significantly affected by TIP-1 knockdown at the mRNA or protein level. Although more studies are needed to elucidate the mechanism(s), TIP-1 likely controls secretion of those angiogenic factors. Several TIP-1-interacting proteins, such as such as β-catenin [7], Rhotekin [9], and ARHGEF16 [12], are directly or indirectly involved in the activation of Rho GTPases for protein secretion [43; 44]. Roles of TIP-1 in the glioblastoma formation and growth and its proposed mechanisms of action were summarized in Fig. 7.

In conclusion, this study revealed a novel role of TIP-1 in tumor formation, angiogenesis, fibronectin expression and secretion of angiogenic factors of human glioblastoma. TIP-1 knockdown with RNA interference significantly delayed tumor formation of human glioblastoma cell lines in animal models. Therefore, it would be judicious to further study the biological relevance and the mechanism(s) of action of TIP-1 expression in the initiation, aggressive growth and treatment response of human glioblastoma.

Supplementary Material

Refer to Web version on PubMed Central for supplementary material.

Acknowledgments

This study was supported in part by NIH grants R01CA127482 (Z Han) and P50 CA128323 (J Gore). NIH has no roles in the study design and data collection, analysis and interpretation or presentation. We are grateful to the kind help on GBM xenograft cell lines from Drs. Jeremy Rich (Cleveland Clinics) and Jialiang Wang (Neurosurgery,

Vanderbilt University). We appreciate the technical assistance and advice from Dr. Ling Geng (Pathology, Vanderbilt University) in the animal studies, Dr. Bret Mobley (Pathology, Vanderbilt University) in the microscopic examination of tissue blocks, and the technical staffs at the Cell Imaging, Histology, and Genomics Cores at the Vanderbilt-Ingram Cancer Center.

References

[1]. Van Meir EG, Hadjipanayis CG, Norden AD, Shu HK, Wen PY, Olson JJ. Exciting new advances in neuro-oncology: the avenue to a cure for malignant glioma. CA Cancer J Clin. 2010; 60:166–193. [PubMed: 20445000]

[2]. Bredel M, Scholtens DM, Yadav AK, Alvarez AA, Renfrow JJ, Chandler JP, Yu IL, Carro MS, Dai F, Tagge MJ, Ferrarese R, Bredel C, Phillips HS, Lukac PJ, Robe PA, Weyerbrock A, Vogel H, Dubner S, Mobley B, He X, Scheck AC, Sikic BI, Aldape KD, Chakravarti A, Harsh G.R.t. NFKBIA deletion in glioblastomas. N Engl J Med. 2011; 364:627–637. [PubMed: 21175304]

[3]. Parsons DW, Jones S, Zhang X, Lin JC, Leary RJ, Angenendt P, Mankoo P, Carter H, Siu IM, Gallia GL, Olivi A, McLendon R, Rasheed BA, Keir S, Nikolskaya T, Nikolsky Y, Busam DA, Tekleab H, Diaz LA Jr. Hartigan J, Smith DR, Strausberg RL, Marie SK, Shinjo SM, Yan H, Riggins GJ, Bigner DD, Karchin R, Papadopoulos N, Parmigiani G, Vogelstein B, Velculescu VE, Kinzler KW. An integrated genomic analysis of human glioblastoma multiforme. Science (New York, N.Y. 2008; 321:1807–1812.

[4]. Comprehensive genomic characterization defines human glioblastoma genes and core pathways. Nature. 2008; 455:1061–1068. [PubMed: 18772890]

[5]. Phillips HS, Kharbanda S, Chen R, Forrest WF, Soriano RH, Wu TD, Misra A, Nigro JM, Colman H, Soroceanu L, Williams PM, Modrusan Z, Feuerstein BG, Aldape K. Molecular subclasses of high-grade glioma predict prognosis, delineate a pattern of disease progression, and resemble stages in neurogenesis. Cancer Cell. 2006; 9:157–173. [PubMed: 16530701]

[6]. Besser J, Leito JT, van der Meer DL, Bagowski CP. Tip-1 induces filopodia growth and is important for gastrulation movements during zebrafish development. Dev Growth Differ. 2007; 49:205–214. [PubMed: 17394599]

[7]. Kanamori M, Sandy P, Marzinotto S, Benetti R, Kai C, Hayashizaki Y, Schneider C, Suzuki H. The PDZ protein tax-interacting protein-1 inhibits beta-catenin transcriptional activity and growth of colorectal cancer cells. J Biol Chem. 2003; 278:38758–38764. [PubMed: 12874278]

[8]. Zencir S, Ovee M, Dobson MJ, Banerjee M, Topcu Z, Mohanty S. Identification of brain-specific angiogenesis inhibitor 2 as an interaction partner of glutaminase interacting protein. Biochem Biophys Res Commun. 2011; 411:792–797. [PubMed: 21787750]

[9]. Reynaud C, Fabre S, Jalinot P. The PDZ protein TIP-1 interacts with the Rho effector rhotekin and is involved in Rho signaling to the serum response element. J Biol Chem. 2000; 275:33962–33968. [PubMed: 10940294]

[10]. Hampson L, Li C, Oliver AW, Kitchener HC, Hampson IN. The PDZ protein Tip-1 is a gain of function target of the HPV16 E6 oncoprotein. Int J Oncol. 2004; 25:1249–1256. [PubMed: 15492812]

[11]. Rousset R, Fabre S, Desbois C, Bantignies F, Jalinot P. The C-terminus of the HTLV-1 Tax oncoprotein mediates interaction with the PDZ domain of cellular proteins. Oncogene. 1998; 16:643–654. [PubMed: 9482110]

[12]. Oliver AW, He X, Borthwick K, Donne AJ, Hampson L, Hampson IN. The HPV16 E6 binding protein Tip-1 interacts with ARHGEF16, which activates Cdc42. Br J Cancer. 2011; 104:324–331. [PubMed: 21139582]

[13]. Alewine C, Olsen O, Wade JB, Welling PA. TIP-1 Has PDZ Scaffold Antagonist Activity. Mol Biol Cell. 2006; 17:4200–4211. [PubMed: 16855024]

[14]. Olalla L, Aledo JC, Bannenberg G, Marquez J. The C-terminus of human glutaminase L mediates association with PDZ domain-containing proteins. FEBS Lett. 2001; 488:116–122. [PubMed: 11163757]

[15]. Han M, Wang H, Zhang HT, Han Z. The PDZ protein TIP-1 facilitates cell migration and pulmonary metastasis of human invasive breast cancer cells in athymic mice. Biochem Biophys Res Commun. 2012; 422:139–145. [PubMed: 22564736]

[16]. Wang H, Yan H, Fu A, Han M, Hallahan D, Han Z. TIP-1 translocation onto the cell plasma membrane is a molecular biomarker of tumor response to ionizing radiation. PloS one. 2010; 5:e12051. [PubMed: 20711449]

[17]. Felgner PL, Gadek TR, Holm M, Roman R, Chan HW, Wenz M, Northrop JP, Ringold GM, Danielsen M. Lipofection: a highly efficient, lipid-mediated DNA-transfection procedure. Proc Natl Acad Sci U S A. 1987; 84:7413–7417. [PubMed: 2823261]

[18]. Ozawa T, James CD. Establishing Intracranial Brain Tumor Xenografts With Subsequent Analysis of Tumor Growth and Response to Therapy using Bioluminescence Imaging. J. Vis. Exp. 2010; 41:5.

[19]. Bonfil RD, Vinyals A, Bustuoabad OD, Llorens A, Benavides FJ, Gonzalez-Garrigues M, Fabra A. Stimulation of angiogenesis as an explanation of Matrigel-enhanced tumorigenicity. Int J Cancer. 1994; 58:233–239. [PubMed: 7517919]

[20]. Zeeberg BR, Feng W, Wang G, Wang MD, Fojo AT, Sunshine M, Narasimhan S, Kane DW, Reinhold WC, Lababidi S, Bussey KJ, Riss J, Barrett JC, Weinstein JN. GoMiner: a resource for biological interpretation of genomic and proteomic data. Genome Biol. 2003; 4:R28. [PubMed: 12702209]

[21]. Sun L, Hui AM, Su Q, Vortmeyer A, Kotliarov Y, Pastorino S, Passaniti A, Menon J, Walling J, Bailey R, Rosenblum M, Mikkelsen T, Fine HA. Neuronal and glioma-derived stem cell factor induces angiogenesis within the brain. Cancer Cell. 2006; 9:287–300. [PubMed: 16616334]

[22]. Reiner A, Yekutieli D, Benjamini Y. Identifying differentially expressed genes using false discovery rate controlling procedures. Bioinformatics (Oxford, England). 2003; 19:368–375.

[23]. Freije WA, Castro-Vargas FE, Fang Z, Horvath S, Cloughesy T, Liau LM, Mischel PS, Nelson SF. Gene expression profiling of gliomas strongly predicts survival. Cancer Res. 2004; 64:6503–6510. [PubMed: 15374961]

[24]. Arnaoutova I, Kleinman HK. In vitro angiogenesis: endothelial cell tube formation on gelled basement membrane extract. Nat Protoc. 2010; 5:628–635. [PubMed: 20224563]

[25]. Staton CA, Reed MW, Brown NJ. A critical analysis of current in vitro and in vivo angiogenesis assays. Int J Exp Pathol. 2009; 90:195–221. [PubMed: 19563606]

[26]. Astrof S, Hynes RO. Fibronectins in vascular morphogenesis. Angiogenesis. 2009; 12:165–175. [PubMed: 19219555]

[27]. Avraamides CJ, Garmy-Susini B, Varner JA. Integrins in angiogenesis and lymphangiogenesis. Nat Rev Cancer. 2008; 8:604–617. [PubMed: 18497750]

[28]. Jogie-Brahim S, Feldman D, Oh Y. Unraveling insulin-like growth factor binding protein-3 actions in human disease. Endocr Rev. 2009; 30:417–437. [PubMed: 19477944]

[29]. Apte SS. A disintegrin-like and metalloprotease (reprolysin-type) with thrombospondin type 1 motif (ADAMTS) superfamily: functions and mechanisms. J Biol Chem. 2009; 284:31493–31497. [PubMed: 19734141]

[30]. Anborgh PH, Mutrie JC, Tuck AB, Chambers AF. Role of the metastasis-promoting protein osteopontin in the tumour microenvironment. J Cell Mol Med. 2010; 14:2037–2044. [PubMed: 20597997]

[31]. Gimbrone MA Jr. Leapman SB, Cotran RS, Folkman J. Tumor dormancy in vivo by prevention of neovascularization. J Exp Med. 1972; 136:261–276. [PubMed: 5043412]

[32]. Olalla L, Gutierrez A, Jimenez AJ, Lopez-Tellez JF, Khan ZU, Perez J, Alonso FJ, de la Rosa V, Campos-Sandoval JA, Segura JA, Aledo JC, Marquez J. Expression of the scaffolding PDZ protein glutaminase-interacting protein in mammalian brain. Journal of neuroscience research. 2008; 86:281–292. [PubMed: 17847083]

[33]. Ribatti D, Leali D, Vacca A, Giuliani R, Gualandris A, Roncali L, Nolli ML, Presta M. In vivo angiogenic activity of urokinase: role of endogenous fibroblast growth factor-2. Journal of cell science. 1999; 112(Pt 23):4213–4221. [PubMed: 10564640]

[34]. Plouet J, Moro F, Bertagnolli S, Coldeboeuf N, Mazarguil H, Clamens S, Bayard F. Extracellular cleavage of the vascular endothelial growth factor 189-amino acid form by urokinase is required for its mitogenic effect. The Journal of biological chemistry. 1997; 272:13390–13396. [PubMed: 9148962]

[35]. Sozzani S, Rusnati M, Riboldi E, Mitola S, Presta M. Dendritic cell-endothelial cell cross-talk in angiogenesis. Trends in immunology. 2007; 28:385–392. [PubMed: 17692569]

[36]. Granata R, Trovato L, Lupia E, Sala G, Settanni F, Camussi G, Ghidoni R, Ghigo E. Insulin-like growth factor binding protein-3 induces angiogenesis through IGF-I- and SphK1-dependent mechanisms. J Thromb Haemost. 2007; 5:835–845. [PubMed: 17388800]

[37]. Wang J, Wakeman TP, Lathia JD, Hjelmeland AB, Wang XF, White RR, Rich JN, Sullenger BA. Notch promotes radioresistance of glioma stem cells. Stem Cells. 2010; 28:17–28. [PubMed: 19921751]

[38]. Wang J, Wang H, Li Z, Wu Q, Lathia JD, McLendon RE, Hjelmeland AB, Rich JN. c-Myc is required for maintenance of glioma cancer stem cells. PloS one. 2008; 3:e3769. [PubMed: 19020659]

[39]. Gradl D, Kuhl M, Wedlich D. The Wnt/Wg signal transducer beta-catenin controls fibronectin expression. Mol Cell Biol. 1999; 19:5576–5587. [PubMed: 10409747]

[40]. Bielefeld KA, Amini-Nik S, Whetstone H, Poon R, Youn A, Wang J, Alman BA. Fibronectin and beta-catenin act in a regulatory loop in dermal fibroblasts to modulate cutaneous healing. J Biol Chem. 2011; 286:27687–27697. [PubMed: 21652705]

[41]. Michaelson JE, Ritzenthaler JD, Roman J. Regulation of serum-induced fibronectin expression by protein kinases, cytoskeletal integrity, and CREB. American journal of physiology. Lung cellular and molecular physiology. 2002; 282:L291–301. [PubMed: 11792634]

[42]. Dean DC, McQuillan JJ, Weintraub S. Serum stimulation of fibronectin gene expression appears to result from rapid serum-induced binding of nuclear proteins to a cAMP response element. J Biol Chem. 1990; 265:3522–3527. [PubMed: 2137458]

[43]. Carlin LM, Evans R, Milewicz H, Fernandes L, Matthews DR, Perani M, Levitt J, Keppler MD, Monypenny J, Coolen T, Barber PR, Vojnovic B, Suhling K, Fraternali F, Ameer-Beg S, Parker PJ, Thomas NS, Ng T. A Targeted siRNA Screen Identifies Regulators of Cdc42 Activity at the Natural Killer Cell Immunological Synapse. Sci Signal. 2011; 4:ra81. [PubMed: 22126964]

[44]. Wang C, Yoo Y, Fan H, Kim E, Guan KL, Guan JL. Regulation of Integrin beta 1 recycling to lipid rafts by Rab1a to promote cell migration. J Biol Chem. 2010; 285:29398–29405. [PubMed: 20639577]

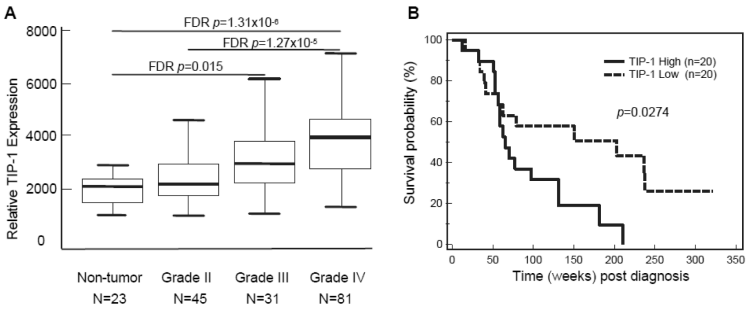

Fig. 1.

Elevated TIP-1 expression levels correlate with the poor prognosis of human glioblastomas. (A) Relative TIP-1 expression levels in human malignant gliomas of various stages upon WHO grading standard. The data distribution was presented as box plot. Note the correlation of the TIP-1 expression levels with the pathological grades of tumors. (B) Kaplan-Meier survival curve to show survival probability of glioblastoma (WHO grade IV) patients after diagnosis is stratified by the TIP-1 expression levels (log-rank analysis, p=0.0274).

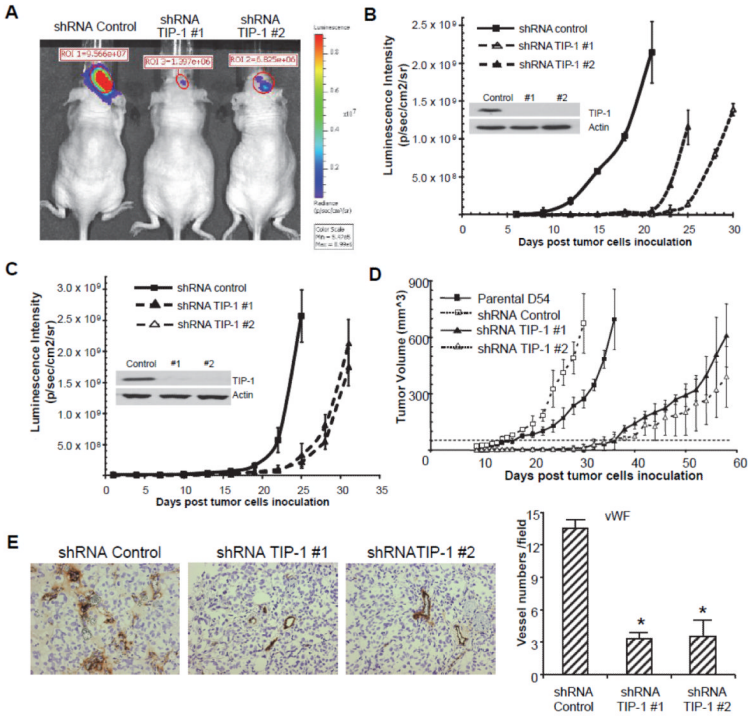

Fig. 2.

TIP-1 knockdown within human glioblastoma cell lines delays tumor formation and impairs angiogenesis in nude mice. D54 or U87 cells were genetically modified with recombinant lentiviruses expressing luciferase and TIP-1-targeted or a control shRNA before the intracranial inoculation. TIP-1 expression in the transfected cells was verified by western blot analyses with a specific antibody (inserts in B & C). Tumor formation and growth were monitored with bioluminescence imaging (BLI) upon luciferase expression. (A) Representative BLI data collected at day 21 post D54 cell inoculation, quantitative measurements of tumor growth were shown upon BLI signal intensity. (B) D54 and (C) The graphs show the time course of tumor formation and growth of D54 (B) and U87 (C) cells in nude mice (n = 5 for each group). (D) Growth curves of D54 tumors in a subcutaneously implanted xenograft model (n=5 for each group). A dashed line indicates tumor size as of 50 mm^3. (E) Tumor-associated blood vessels were visualized with vWF staning (brown) and quantified upon images. Tumors were resected at day 12 post inoculation in a subcutaneously implanted xenograft model. Hematoxylin (blue) was used for counterstaining. Quantification was based upon more than 12 independent microscopic fields for each group. Shown are mean +/− SD. * $p<0.05$ compared to the shRNA control by the Student's *t*-test.

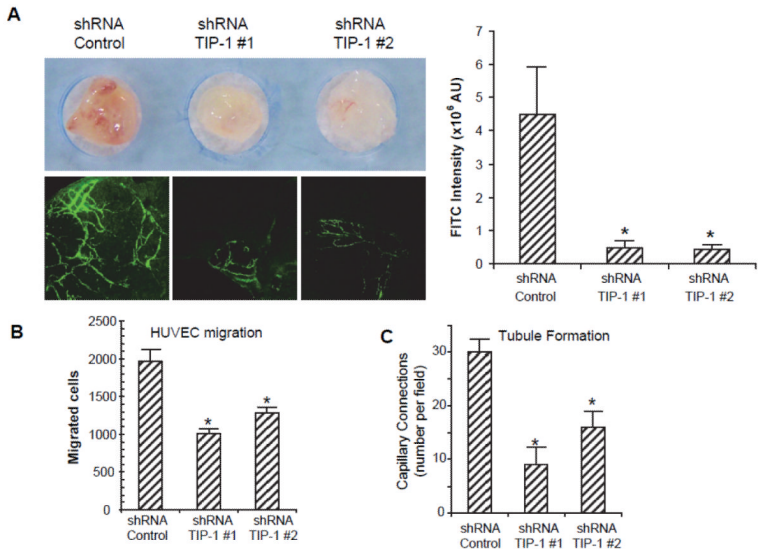

Fig. 3.

TIP-1 knockdown impairs production of angiogenic factors within D54 cells. (A) Matrigel-plug assays. A half million D54 cells with or without TIP-1 knockdown were mixed with matrigel for subcutaneous implantation in nude mice. FITC-dextran was injected into the tail vein on day 8 after the matrigel plug implantation. Tumors were resected for examination with a confocal fluorescence microscope. Shown are representative images and quantitative measurement (ImageJ) of the FITC signals from at least 12 microscopic fields. * $p<0.05$ compared to the shRNA control. (B) Angiogenic activity of pre-conditioned medium from monolayer culture of D54 cells was analyzed with a Boyden chamber-based HUVEC migration assay. Shown are the means ± SDs of three experiments in which HUVECs migrated through the porous chambers. (C) HUVEC tubule formation assay using pre-conditioned medium from monolayer culture of D54 cells. Shown are the quantitative measurements of capillary connections with more than 3 branches. Bars represent the means ± SDs of three independent experiments. * $p<0.05$ compared to the shRNA control by the Student's *t*-test.

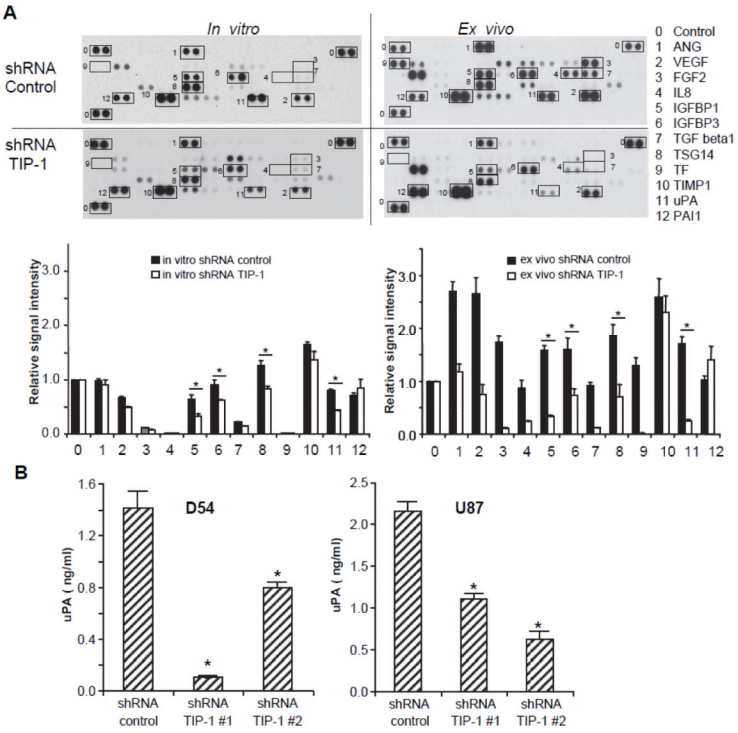

Fig. 4.

TIP-1 knockdown suppresses secretion of angiogenic factors from glioblastoma cells. (A) Angiogenic factors in the D54 pre-conditioned medium were detected with a Human Angiogenesis Antibody Array kit. Shown are representative images of three independent experiments and quantitative measurements of the mean signal intensity of each spot with ImageJ. Identity of each arrayed antibodies is indicated in the legend at right. * $p<0.05$. (B) uPA in the pre-conditioned medium was measured with an ELISA kit, the optical density was converted to uPA concentration based on the titration results with a standard control. Shown are the means ± SDs from three experiments in D54 (left) and U87 (right) cells with or without TIP-1 knockdown. * $p<0.05$ compared to the controls by the Student's t-test.

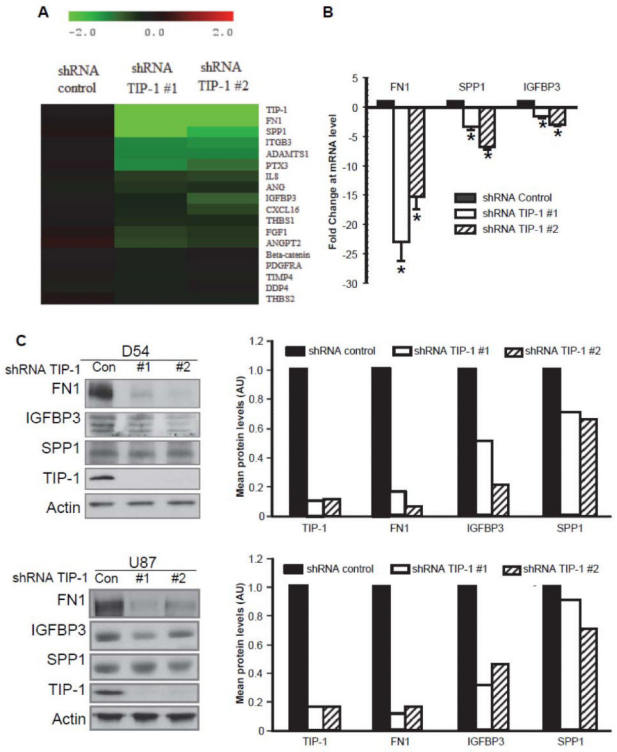

Fig. 5.

TIP-1 knockdown reduces fibronectin expression in glioblastoma cells. (A) Heatmap showing the expression levels of some angiogenesis-related genes within D54 cells with or without TIP-1 knockdown. TIP-1 was included to show the efficiency of TIP-1 knockdown. (B) Quantitative RT-PCR analyses of FN1, SPP1 and IGFBP3 gene expression within D54 cells. Shown are fold changes at mRNA level of each gene, compared to that in the control cells (set to a value of 1). Means ± SDs from three indepdendent experiments. * $p<0.05$ compared to the shRNA control by the Student's *t*-test. (C) Western blot analyses and semi-quantification of FN1, IGFBP3 and SPP1 protein levels in human glioblastoma cell lines D54 and U87. TIP-1 and actin were blotted as controls. Intensity of the protein bands was analyzed with ImageJ and normalized to the loading control (actin). The expression level of each protein was normalized upon those in the control cells (set to a value of 1).

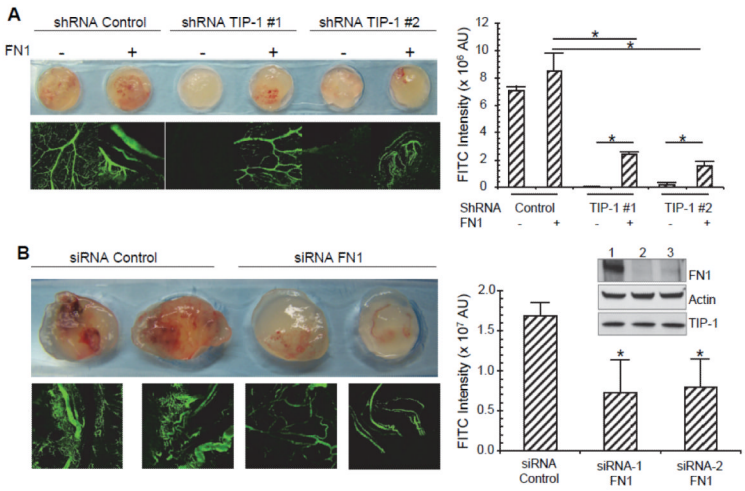

Fig. 6.

FN1 is involved in the TIP-1-regulated angiogenesis in human glioblastomas. (A) D54 cells with or without TIP-1 knockdown were mixed with 25 μg/ml of recombinant FN1 protein or PBS control for the matrigel-plug assays. Tumor blood vessels within the matrigel-plugs were detected and quantified at day 8 after plug implantation as described in *Materials and Methods*. $p<0.05$, n=5. The Student's *t*-test. (B) FN1 expression within D54 cells was down-regulated with two validated siRNAs against human FN1 transcripts. The efficiency of siRNA was detected with western blot analyses with specific antibodies (lane 1, control siRNA; lane 2, FN1 siRNA #1; and lane 3, FN1 siRNA #2) as shown in the insert. The transfected cells were used for the matrigel-plug assays 72 hours post-transfection. Shown are representative images and quantitative measurements of fluorescence intensity (ImageJ). * $p<0.05$ compared to controls by the Student's *t*-test.

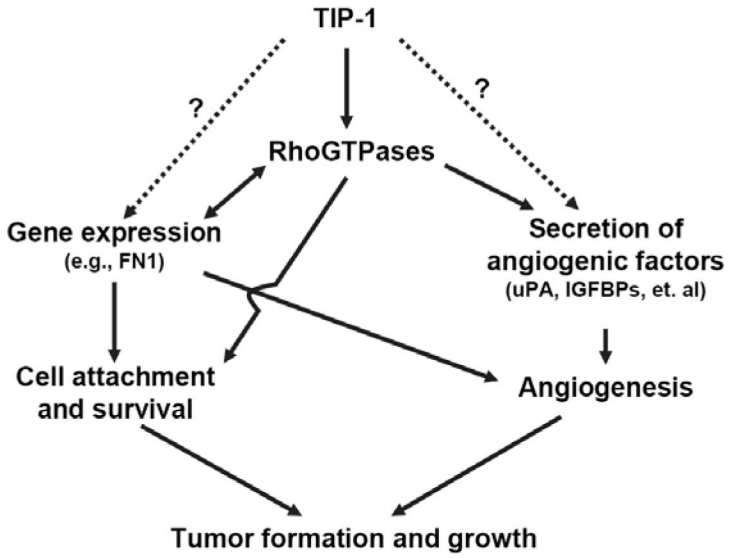

Fig. 7.

B>. Schematic illustration of TIP-1's roles in the formation and growth of glioblastoma. Solid lines indicate documented pathways, while dashed lines show putative pathways to be explored.